ELSEVIER

Ultramicroscopy 70 (1997) 45–55

ultramicroscopy

Non-contact scanning probe microscopy with sub-piconewton force sensitivity

Takaaki Aoki[a], Michio Hiroshima[a], Kazuo Kitamura[a,b], Makio Tokunaga[b], Toshio Yanagida[a,b,c,*]

[a] *Department of Biophysical Engineering, Osaka University, Machikaneyama 1-3, Toyonaka, Osaka 560, Japan*

[b] *BioMotron Project, Exploratory Research for Advanced Technology, Japan Science and Technology Corporation, Senba-Higashi 2-4-14, Mino, Osaka 562, Japan*

[c] *Department of Physiology, Osaka University Medical School, Yamadaoka 2-2, Suita, Osaka 565, Japan*

Received 24 April 1997; received in revised form 10 July 1997

Abstract

Aiming at detecting and visualizing weak interaction forces between biological macromolecules in non-contact mode, we have refined scanning probe microscopy to have approximately 100-fold higher sensitivity than conventional atomic force microscopy (AFM). The essential features of this system are that the force sensitivity is in the sub-piconewton range and the gap distance between interacting stylus and the sample surfaces can be controlled with nanometer accuracy. We have achieved these technical improvements by using flexible handmade cantilevers with the spring constant of approximately 0.1 pN nm^{-1}. Thermal bending motions have been reduced to less than 1 nm in root-mean-square amplitude by exerting feedback forces with a laser radiation pressure. The performance of this newly developed scanning probe microscopy was tested by measuring electrostatic repulsive forces in solution. Intermolecular forces in the sub-piconewton range were resolved at controlled gaps in the nanometer range between an amino-silanized stylus and an amino-silanized glass surface. Force curves as a function of gap distance coincided well with the theory of electricity. Debye lengths calculated at various ionic strengths were in good agreement with the Debye–Hückel theory. Furthermore, non-contact two-dimensional images mapped with electrostatic forces within the piconewton range could also be obtained. This system should prove useful not only for constructing the surface topographies of soft biomaterials but also for mapping the surfaces with intermolecular forces which are closely related to their functions.

PACS: 07.79.L; 34.20.G; 87.64.D

Keywords: Flexible cantilevers; Feedback control; Radiation pressure; Electrostatic interactions

* Corresponding author. Tel.: 81-6-850-6510; fax: 81-6-857-5421; e-mail: yanagida@bpe.es.osaka-u.ac.jp.

PII S0304-3991(97)00069-7

1. Introduction

Atomic force microscopy (AFM) developed in 1986 [1] is a powerful tool to visualize fine surface structures and has proved particularly useful in the field of material science. AFM was also expected to be a promising tool for biological applications because it does not choose measurement atmospheres and specimens do not necessarily have to be conductive. Therefore, AFM has been widely used in biological materials [2]. However, measurements of biological macromolecules surface structures with AFM have met with serious technical problems. The major problem is that atomic forces operate within a distance of 1 nm between the probe stylus and the material surface, so fragile biological macromolecules are easily collapsed with stiff stylus tips and the images of the surfaces are influenced by the shape of stylus tip. Rather than to visualize the surface structures of biomaterials, AFM has been recently used in contact mode to measure the breaking forces between complexes of biological molecules, such as biotin-avidin [3, 4] and complementary DNA pairs [5], and the forces due to shape changes of protein molecules during enzymatic reaction [6, 7].

The aim of this work is to develop high sensitivity scanning microscopy that enables us to visualize intermolecular interactions in non-contact mode between single biological molecules such as protein–protein, protein–nucleic acid, ligand–receptor, by improving the force sensitivity of AFM. Recently, remarkable progress has been made in developing techniques for manipulation and nanometry of single biological macromolecules using glass microneedles or an optical trap. These techniques have enabled one to directly measure forces caused by interactions between motor proteins [8–11] or between DNA and RNA polymerase [12]. The observed forces are several piconewtons. They are much smaller than that detectable with conventional AFM, which is in the range of nanonewton. Interaction forces in non-contact region would be even smaller than these forces.

In order to detect such weak interaction forces in non-contact mode, we have used highly sensitive handmade cantilevers with a spring constant of the order of 0.1 pN nm^{-1}, which is over 100-fold more flexible than commercialized cantilevers typically used in conventional AFM. The flexible cantilevers, however, undergo large Brownian motions. This problem has been overcome by exerting feedback forces with laser radiation pressure. To test the performance of this novel probe microscopy, electrostatic repulsive forces between a positively charged stylus and a glass surface in solution were measured. The system allowed us to map a non-contact two-dimensional force profile of the material surface with electrostatic forces in the piconewton range. These results showed that the newly developed system could resolve sub-piconewton intermolecular forces, controlling the gaps between stylus and material surface in the nanometer range.

Preliminary results have been previously published elsewhere [13].

2. Materials and methods

2.1. Preparation of very flexible cantilevers

A thin coverslip (24 mm × 32 mm, 30 μm in thickness; a custom made item; Matsunami Glass, Osaka, Japan) was cut into narrow strips (5 mm × 24 mm) with a diamond cutter. The strips of glass were then heated and extended with a capillary puller (PD-5; Narishige, Tokyo, Japan) to a width of 20 μm and a thickness of 0.2 μm. The extended thin glass sheets were attached to a glass base (5 mm × 5 mm × 0.2 mm) with an epoxy bonding agent and cut to 200–300 μm in length with a pair of ophthalmic scissors under a binocular microscope (SZH-10; Olympus Optical, Tokyo, Japan). The upper side of the thin glass sheet was coated with gold using a vacuum evaporator (JEE-400; JEOL, Tokyo, Japan) to reflect laser beams. The thickness of the gold film was approximately 300 Å. In order to prevent warp of the cantilevers during the gold coating procedure, the coated region was limited to an area 0 to 50–100 μm from the front edge. A very sharp ZnO whisker crystal (gift from Matsushita Electric Industrial Co., Osaka, Japan), which has a high aspect ratio (cone half angle of 1–2°) and a small radius of curvature at the tip summit (less than 10 nm) [14, 15], was then

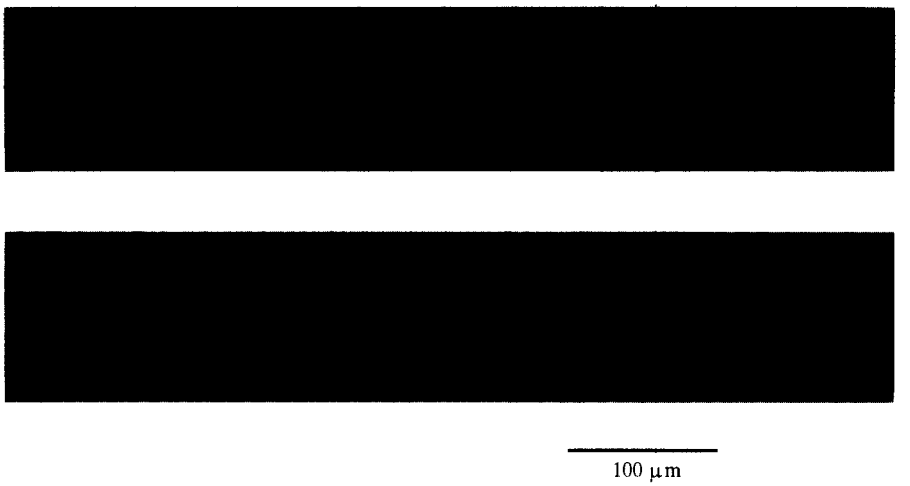

Fig. 1. Optical microscopic images of a handmade cantilever with a stiffness of approximately 0.1 pN nm^{-1}. Upper and lower panels show the top and the side views, respectively.

attached to the other side by the epoxy bonding agent under the binocular microscope (Fig. 1). As the length of whisker leg varied from several microns to over a hundred microns [16], we chose a whisker crystal with a leg length of approximately 10 μm as a probe stylus. This cantilever was attached to a lever holder of a conventional AFM with nail polish.

The stiffness of the cantilevers were determined by two methods; (1) cross-calibration against a standard glass microneedle of known stiffness by essentially the same methods described previously [17], (2) by measuring the thermal bending motions of the cantilevers in water [9]. Mean square displacement of the thermal vibrations of a cantilever ($\langle z^2 \rangle$), obtained as the integral of power spectral density (PSD), should be combined with the stiffness of the cantilever by the principle of equipartition, $1/2k_BT = 1/2\, K\langle z^2 \rangle$, where k_B is the Boltzmann constant, T is the absolute temperature, and K is the stiffness of the cantilever. The values determined by both methods were consistent with each other (Fig. 2).

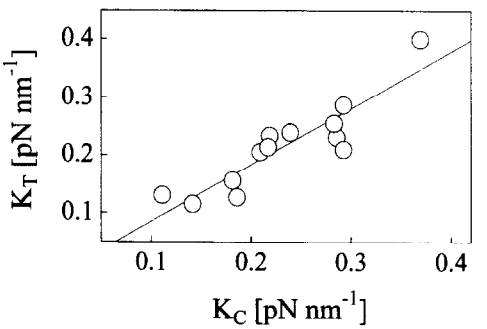

Fig. 2. Comparison of the stiffness values of the cantilevers determined by two different methods. K_C, stiffness determined by cross-calibration method; K_T, stiffness determined by thermal fluctuation analysis. See text for details.

2.2. Position control of a cantilever with laser radiation pressure

Fig. 3 shows schematic diagram of the apparatus. The setup was constructed on a conventional liquid–type AFM (NV2000; Olympus Optical), and was positioned on a vibration-free table (HG-107LM; Herz, Tokyo, Japan). A laser beam for position sensing (L1, $\lambda = 780$ nm, 3 mW diode laser, component of NV2000 system) was reflected with a dichroic mirror, DM1 ($\lambda > 720$ nm reflected, a custom made item; Olympus Optical) and was focused onto the back surface of a cantilever through a water immersion objective lens (WPlanFL40 × UV; Olympus Optical). The reflected beam was projected into quadrant photodiodes and the height position of the cantilever was

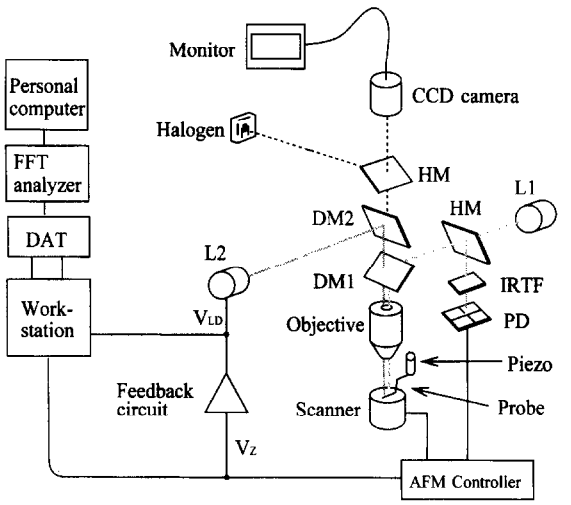

Fig. 3. Schematic diagram of an experimental setup. L1, L2, laser diodes; DM1, DM2, dichroic mirrors; HM, half mirrors; IRTF, infrared transmission filter; PD, photodiodes; V_Z, height signal of cantilevers; V_{LD}, input signal to L2. See text for details.

determined by the focusing error detection method [18]. An infrared transmission filter ($\lambda > 750$ nm transmitted, a custom made item; Asahi spectra, Tokyo, Japan) was placed in front of the photodiodes to reject scattered light. The height signal was amplified and modulated by a feedback circuit (a custom made item, commercially available as CF201; Sentech, Hirakata, Osaka, Japan).

Another laser beam with 680 nm wavelength (L2, 20 mW diode laser, IMSO601A; Panasonic, Osaka, Japan) was used for position controlling. Its intensity was modulated by the output signal V_{LD} of the feedback circuit (see Section 2.3.). The laser beam (L2) was reflected with a dichroic mirror (DM2, DM605; Asahi Spectra) and was focused onto the cantilever through an objective lens. To avoid extreme temperature gradient due to local illumination onto the probe caused by high energy density of the laser beam (L2), the spot of the beam on the back surface of cantilevers was slightly defocused to illuminate an area approximately 20 μm × 20 μm. The effect of illumination with the beam (L2) to position sensing was below the detection limit. The height signal (V_z) and feedback signal (V_{LD}) were monitored with a digital storage oscilloscope (CS-8010; Kenwood, Tokyo, Japan) and recorded on tape with a digital data recorder (RD-120TE; TEAC, Tokyo, Japan) at a sampling rate of 24 kHz. The data were analyzed off-line with a fast Fourier transform (FFT) analyzer (R9211A; Advantest, Tokyo, Japan) and with a personal computer (4266DX; Canon, Tokyo, Japan). Image data by AFM were recorded with a workstation (Apollo 9000; Hewlett Packard, Palo Alto, CA). The optical microscopic images of the probes and samples were displayed on a TV monitor (PM-121T; Ikegami, Tokyo, Japan) with a CCD camera (CS5110; Tokyo Electronic, Tokyo, Japan) using a reflecting DIC microscope (BH2-UMA; Olympus Optical). A piezo actuator driven with a function generator (FG-273; Kenwood) was mounted on the base of the cantilever.

2.3. Feedback system

Fig. 4 outlines the construction of the feedback system. The difference between the position signal (V_Z) and the reference signal (V_{ZREF}) was amplified with a magnification of ×200 and passed through a low-pass filter (LPF1) with a 50 kHz cutoff frequency. An offset signal (V_{LDOFF}), which was the low frequency component (cutoff frequency: < 1 kHz) of the output signal (V_{LD}), was then added (see Section 3.1.). V_{LD} was lead to the driver of the diode laser L2 for position controlling.

2.4. Calibration and measurement of force

The base of a cantilever with a known stiffness (K) was sinusoidally oscillated by the piezo actuator. The displacement of the tip of the cantilever was recorded and its amplitude (z_0) was measured off-line. After the feedback system was turned on, the sinusoidal displacement of the cantilever tip was canceled to zero, but the feedback voltage (V_{LD}) oscillated sinusoidally. The amplitude V_{LD0} of the oscillation corresponds to the force $K \times z_0$. Therefore, the force F exerted on the cantilever by some interaction between stylus tip and a specimen is obtained as $F = K \times z_0 \times V_{LD}/V_{LD0}$, where V_{LD} is the feedback voltage required to cancel the cantilever displacement during the interaction.

2.5. Amino-silanization of glass coverslips and ZnO whiskers

Coverslips (24 mm × 32 mm) were cleaned by soaking in 0.1 M KOH for a few hours and then ultrasonicated for 10 min. They were rinsed a few times in milli-Q water, soaked in 10 mM HCl for a moment, thoroughly washed in water and finally washed in ethanol a few times. The cleaned coverslips were amino-silanized in ethanol containing 5% (V/V) 3-aminopropyltriethoxysilane (LS-3150; Shin-etsu Chemicals, Tokyo, Japan), 2.9% H_2O, 1.2 mM HCl at 80°C for 1 h. They were washed in water and then ethanol thoroughly, and stored in ethanol. ZnO whiskers were treated by almost the same procedure with the exception of washing procedures before silanization.

2.6. Electrostatic force measurement

Electrostatic repulsive forces between the positively charged surfaces of a stylus and a coverslip were measured. An amino-silanized coverslip was glued with nail polish on the bottom surface of a culture dish (30 mmϕ) and immersed in distilled water or solutions of varying ionic strengths. The coverslip was slowly translated upwards with an AFM scanner at the rate of 5–10 nm s^{-1}. The cantilever position was kept constant until the stylus tip made contact with the surface of the coverslip, but after contact the cantilever was out of feedback control and it was raised upwards at the scanner speed (v). The moment when the stylus contacted the surface was defined as time zero. The gap distance (D) between the summit of the stylus and the surface of the coverslip was calculated as $v \times$ (time). Scanner hysteresis was negligible in the range 0–300 nm and the displacement of the scanner could be approximated to be linear with time. All experiments were performed at 27 ± 1°C.

2.7. Two-dimensional imaging of non-contact force

The surface of a coverslip with striped bumps (15 μm in width, 2 μm in height) made by chemical etching (gift from Drs. A. Ishijima and H. Tanaka) was positively charged by amino-silanization. Its surface was scanned in x–y directions with an amino-silanized ZnO probe stylus, holding the cantilever position constant. Feedback voltages and height positions of the cantilever were recorded digitally and reconstructed to two-dimensional images with NV2000 system.

3. Results

3.1. Position control of a cantilever with laser radiation pressure

In order to improve the force sensitivity, very flexible handmade cantilevers with a stiffness of approximately 0.1 pN nm^{-1} were used. Such flexible levers, however, undergo large thermal bending motions. According to the principle of equipartition, $\sqrt{\langle z_n^2 \rangle} = \sqrt{(k_B T/K)}$, the amplitude of bending motions of a lever with a stiffness of 0.1 pN nm^{-1} is 6.7 nm in terms of root-mean-square (rms) and approximately 40 nm in the peak-to-peak form (within $\pm 3\sigma$ of displacement distribution).

The effect of thermal vibration has been avoided using laser radiation pressure. When a P mW laser beam is incident perpendicularly onto a surface and totally reflected, the force exerted on the surface F is theoretically represented as $F = 2P/c$, so the force exerted by a 1 mW laser onto a cantilever is calculated to be 6.7 pN. The force required to counterbalance a 40 nm displacement of a cantilever with a stiffness of 0.1 pN nm^{-1} is 40 nm × 0.1 pN nm^{-1} = 4 pN. Therefore, the force exerted by a laser beam of several milliwatts is large enough to cancel the thermal bending motion of a cantilever.

Fig. 4 outlines the feedback system to control the thermal bending motions of a cantilever. The height position of the cantilever was measured by the focusing error detection method [18] using a diode laser (L1). The height signal (V_Z) was used as the input to the feedback circuit. L1 is a laser used for position sensing. The output (V_{LD}) from the feedback circuit was used to drive another diode laser (L2) required for position control. Since the laser radiation pressure exerts only a downwards force, the cantilever was held down in

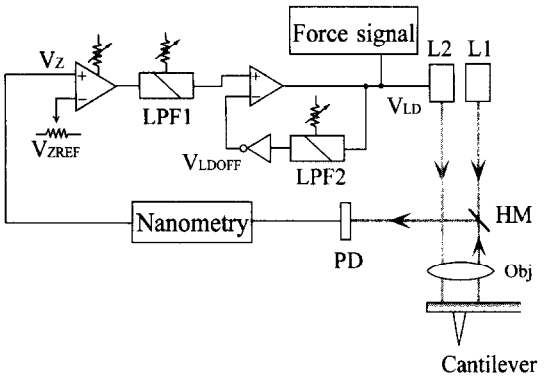

Fig. 4. Schematic diagram of a feedback system using laser radiation pressure. L1, L2, laser diodes; HM, half mirror; PD, photodiode; V_Z, height signal of cantilevers; V_{ZREF}, reference signal for V_Z; V_{LD}, signal for driving L2; V_{LDOFF}, offset of V_{LD}; LPF1, LPF2, low-pass filters. See text for details.

advance by the beam (L2) driven with a signal V_{LDOFF}, unlike the case of optical tweezers [19]. The height was kept constant as follows: if the cantilever fluctuated upwards, a larger force was exerted on the cantilever by increasing the intensity of L2 beam; if it fluctuated downwards, the laser intensity was decreased to weaken the downward force.

The algorithm for this feedback circuit has been modified from the one normally used (Fig. 4). The height signal (V_Z) was amplified 50 to 500 times after the subtraction of reference voltage (V_{ZREF}) that determined the equilibrium cantilever position (z_{REF}). The amplified output signal was passed through a band-pass filter with a cut-off frequency of 50 kHz to minimize electrical and optical noise. After the addition of an offset voltage (V_{LDOFF}), the signal (V_{LD}) was used to drive the laser L2, i. e., $V_{LD} = A(V_Z - V_{ZREF}) + V_{LDOFF}$, where A is the amplifier magnification. As the output signal of optical sensor is linear with the height of the cantilever, V_Z and V_{ZREF} are represented as functions $V_Z = a \times z + b$ and $V_{ZREF} = a \times z_{REF} + b$, where a and b are constants. Therefore, $V_{LD} = Aa(z - z_{REF}) + V_{LDOFF}$. In the case that a constant voltage was used as the offset (V_{LDOFF}), thermal bending motions and displacements due to rapid interaction forces could almost be completely eliminated, but the slow components of positional changes could not be completely reduced when slow or constant force was exerted on the cantilever (data not shown). The slow components of V_{LD} and z, i.e., $\langle V_{LD} \rangle$ and $\langle z \rangle$, are related as $\langle V_{LD} \rangle = Aa(\langle z \rangle - z_{REF}) + V_{LDOFF}$ (note that z_{REF} is constant). In order to keep the cantilever height to z_{REF} constantly, $\langle z \rangle - z_{REF}$ should be equal to zero. Consequently, $V_{LDOFF} = \langle V_{LD} \rangle$ is necessary. Therefore, the slow components $\langle V_{LD} \rangle$ were placed as V_{LDOFF} in a feedback circuit (Fig. 4). The present algorithm has an advantage that the correspondence between z_{REF} and V_{LDOFF} is automatically achieved.

Using this feedback system, the thermal bending motions of the cantilevers were reduced to less than 1 nm in rms. Fig. 5a and Fig. 5b show the thermal bending motions of a cantilever with a stiffness of 0.11 pN nm^{-1} without and with feedback control, respectively. The rms displacement was reduced from 6 to 0.8 nm with feedback control. Fig. 5c shows the power spectral density (PSD) of the thermal bending motions of a cantilever without (upper trace) and with feedback control (middle trace). The upper trace was approximated by a Lorentzian curve with a corner frequency (f_C) of 114 Hz. With feedback control (middle trace), the Lorentzian spectrum component disappeared and the residual small peak in the low-frequency region is practically negligible (of the order of 0.1 nm) after subtraction of the system noise (bottom trace).

Fig. 6a and Fig. 6b show the cantilever positions without and with feedback control, respectively, when external force was exerted onto a cantilever. A sinusoidal oscillation with a peak-to-peak amplitude of 100 nm at a 10 Hz frequency was applied to the base of a cantilever with a stiffness of 0.14 pN nm^{-1}. With feedback control, sinusoidal and thermal bending motions were both reduced to less than 1 nm in rms (Fig. 6b). The force exerted on the cantilever with feedback control was obtained from the feedback voltage V_{LD}. As shown in Fig. 6c, V_{LD} oscillated sinusoidally synchronizing with the applied oscillation. Fig. 6d shows the PSD of cantilever motions without feedback control shown in Fig. 6a, and of the feedback voltage V_{LD} shown in Fig. 6c. The spectrum of V_{LD} has high-frequency components comparable to the spectrum of the cantilever motion (see Section 4), both spectra

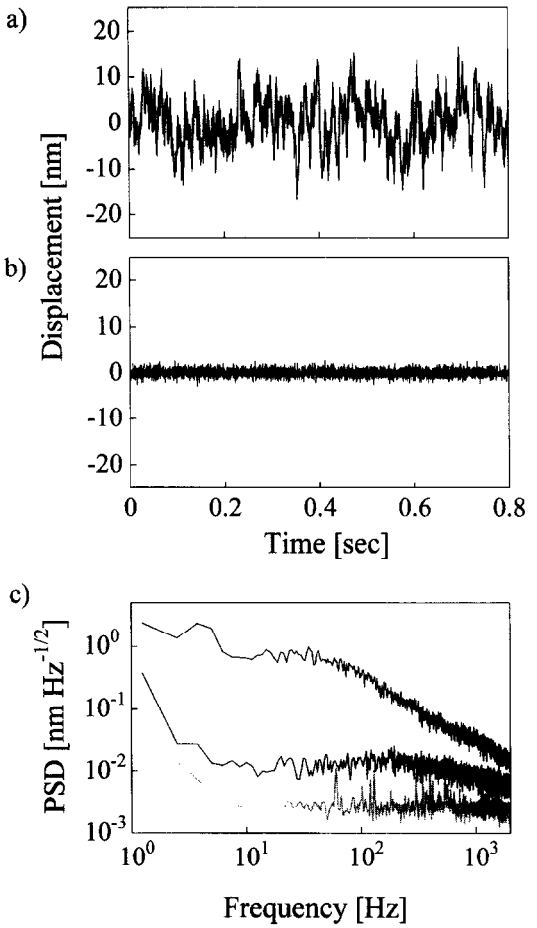

Fig. 5. Thermal bending motions of a cantilever without (a) and with feedback control (b). (c) Power spectral density (PSD) of the cantilever fluctuations shown in (a) (top trace) and (b) (middle trace), and light and electrical noise (bottom trace, gray). The light and electrical noise was measured when the laser beam was reflected at the cantilever base. Displacements were recorded with a 2 kHz cutoff frequency. Cantilever stiffness was 0.11 pN nm^{-1}.

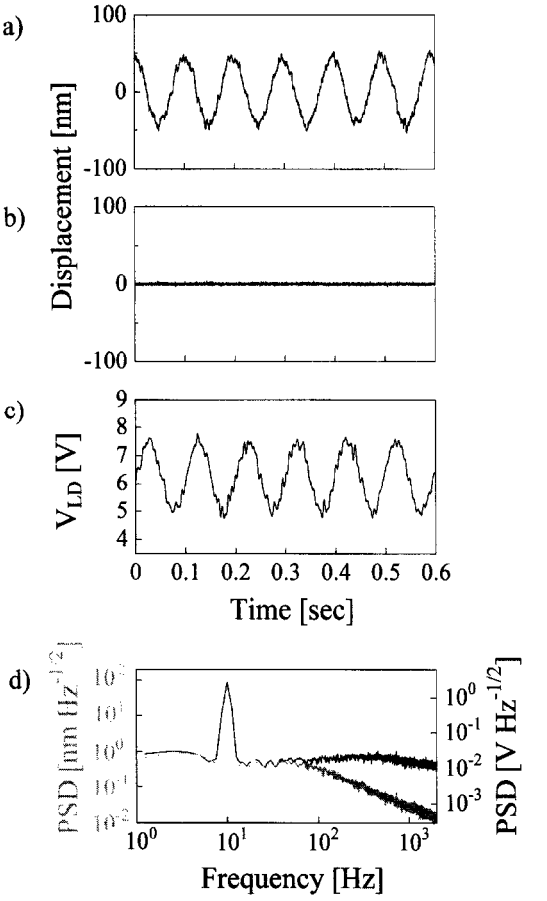

Fig. 6. Control of cantilever positions with the feedback system when the base of a cantilever was oscillated sinusoidally with a peak-to-peak amplitude of 100 nm at a 10 Hz frequency by using a piezo actuator. Displacements in the position of a cantilever tip were measured without (a) and with feedback (b). (c) Output voltage (feedback voltage) V_{LD} delivered from the feedback circuit. (d) PSD of sensor signal (V_Z) without feedback shown in (a) (gray) and of feedback voltage (V_{LD}) with feedback shown in (c) (black). Displacements were recorded with a 2 kHz cutoff frequency in (a) and (b), and with a 100 Hz in (c). Cantilever stiffness was 0.14 pN nm^{-1}

were equivalent within error to each other in the frequency range lower than f_C of the cantilever thermal motion. The good correspondence demonstrates that the force is known accurately from the feedback voltage in the frequency range lower than f_C.

The relationship between the laser power of L2 and the force exerted on a cantilever was demonstrated by changing the amplitude of the sinusoidal oscillations (Fig. 7). The force required to counterbalance the cantilever displacement z was calculated as $z \times K$ (see Section 2.4.). Good linearity was exhibited over the range of 0.4–11 pN. The slope in Fig. 7 was 1.9 pN mW^{-1}, which was smaller than the theoretical value 6.7 pN mW^{-1} when light was totally reflected. However, taking account of a loss of laser power when the beam passes through the dichroic mirrors and the objective lens,

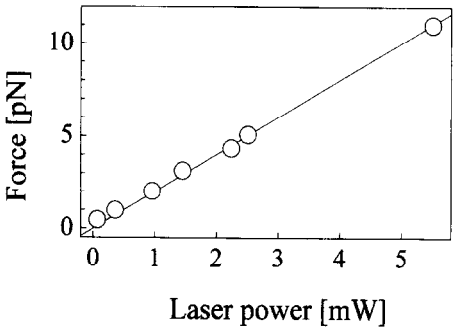

Fig. 7. The relationship between the force applied to a cantilever and laser power output. Various amplitudes (0.3–100 nm) of sinusoidal waves (10 Hz) were applied to the piezo actuator and the forces (absorbed displacement × stiffness, see Fig. 6) were plotted against the power of the position-control laser (L2). Values of feedback voltage (V_{LD}) were obtained from PSD peak values at 10 Hz using an FFT analyzer and converted to laser power by multiplying power/voltage coefficient. Cantilever stiffness was 0.13 pN nm^{-1}.

and of the reflectance of the cantilever gold coating (approximately 80–90%), this value is reasonable.

3.2. Electrostatic force measurement

To test the performance of this novel scanning microscopy, electrostatic repulsive forces between the positively charged surface of a probe stylus and of a coverslip were measured in solution. Amino groups were incorporated onto the surface of the stylus (ZnO whisker) and the coverslip by chemical modification with 3-aminopropyltriethoxysilane.

Fig. 8 shows force versus distance curves at KCl concentrations of 0 mM (a), 0.1 mM (b) and 1 mM (c). The electrostatic force could be considerably reduced by shielding of ionic atmosphere with an increase in the KCl concentration. In the presence of 1 mM KCl, the force was approximately 10 pN around 2 nm and almost zero at a distance of 20 nm (Fig. 8c). The inset of Fig. 8c shows the data averaged over six scans on an expanded force scale. Forces in the range of a piconewton or smaller at a distance of 5 nm could be clearly detected. Thus, this probe microscope system can resolve intermolecular forces of less than one piconewton, and the gap distance between the interacting molecules can be controlled with nanometer accuracy.

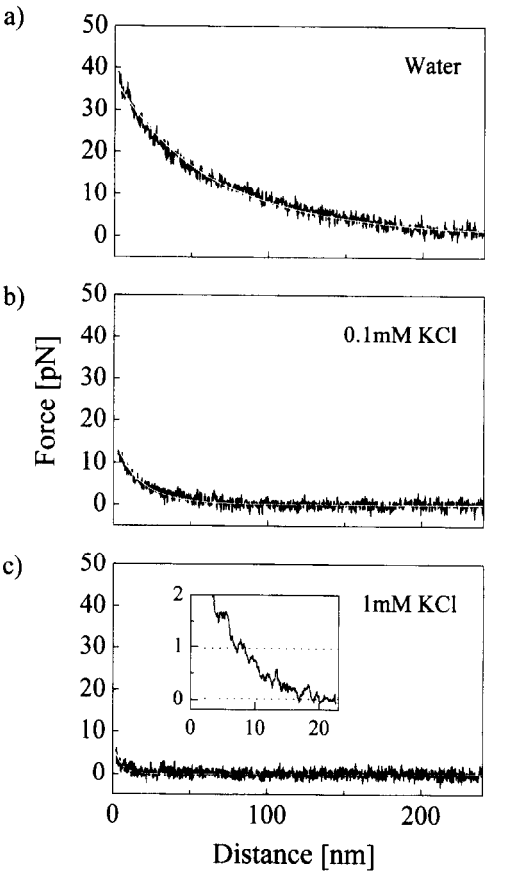

Fig. 8. Electrostatic repulsive forces between positively charged ZnO tip and the glass surface in various solutions are plotted against the gap distance between tip and surface. Solution: (a) water (0 mM KCl), (b) 0.1 mM KCl, (c) 1 mM KCl. Inset: the averaged data for six scans on the expanded force scale. White lines show theoretical force profiles [22] derived by least-square fitting. All data were recorded with a 50 Hz cutoff frequency. Cantilever stiffness was 0.10 pN nm^{-1}.

The force versus distance curves and the dependence on the ionic strength agreed well with the Debye–Hückel theory (Fig. 9, see Section 4).

3.3. Two-dimensional imaging of non-contact force

Two-dimensional non-contact imaging of electrical repulsive forces reflecting the surface features has been achieved (Fig. 10b). The surface of a glass coverslip that had been chemically etched to have striped patterns of 15 μm in width and then amino-silanized was scanned two-dimensionally by

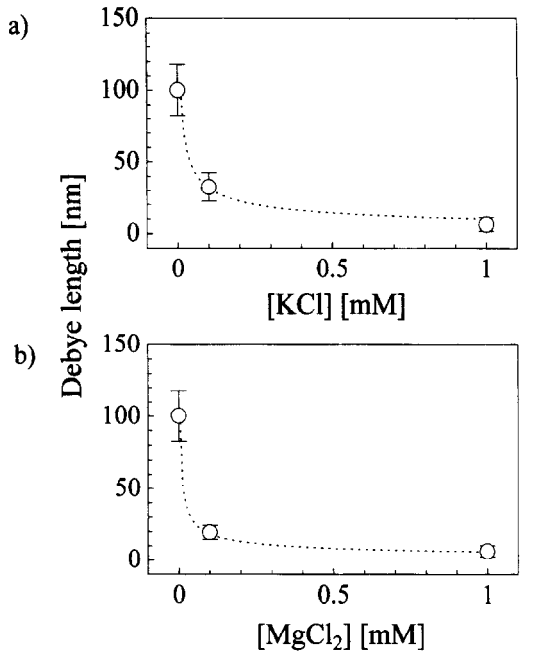

Fig. 9. Salt concentration (C) dependence of Debye length (κ^{-1}) obtained by least-square fitting with theoretical force functions [22] in KCl solution (a) and in $MgCl_2$ solution (b). Dotted lines show theoretical curves for 1 : 1 electrolytes, $\kappa^{-1} = 10.0/\sqrt{C}$ in (a) and for 2 : 1 electrolytes, $\kappa^{-1} = 5.8/\sqrt{C}$ in (b) at 27°C [23].

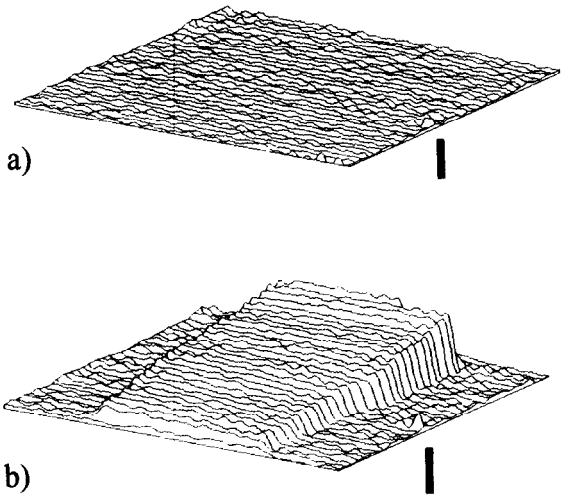

Fig. 10. Two-dimensional image of electrostatic repulsive force measured by non-contact probe microscopy. Simultaneous measurements of the cantilever position (a) and the electrostatic force (measured as feedback voltage, V_{LD}) between stylus and bump (b). Note that the height of the cantilever was not changed during the scanning measurement, so it did not come into contact with the glass surface. The force profile gradient depend on Y axis is caused from the slope of the specimen itself. Scan area was 30 μm × 30 μm and scan rate was 4 s line^{-1}. Scale bar: 5 nm (a) and 10 pN (b). Cantilever stiffness was 0.25 pN nm^{-1}.

an amino-silanized stylus, with the cantilever position being controlled by the feedback system. As shown in Fig. 10a, the height position of the cantilever was kept constant although the electrostatic force changed during scanning. The result demonstrates that the present microscopic system can two-dimensionally map the surface features by measuring intermolecular forces in the piconewton range, keeping out of contact.

4. Discussion

Non-contact scanning probe microscopy with sub-piconewton force resolution has been developed. It was achieved by two novel techniques: (1) handmade cantilevers with very small stiffness, 0.1 pN nm^{-1}, which is over 100-fold more flexible than that typically used in conventional AFM; (2) control of the height position of the cantilever by exerting feedback positioning with laser radiation pressure.

Flexible cantilevers with a stiffness of 0.1 pN nm^{-1} has enabled us to achieve force resolution of the order of sub-piconewton. The displacement of the cantilever is measured at sub-nanometer resolution and the force is obtained as (displacement) × (stiffness), so the force resolution is better than 1 nm × 0.1 pN nm^{-1} = 0.1 pN.

Furthermore, the more flexible the cantilever is, the greater the signal-to-noise ratio. Suppose that we measure the force F by a cantilever with a stiffness of K. The displacement (z) caused by the force (F) is given as $z = F/K$. According to the principle of equipartition, $1/2\, K\langle z_n^2\rangle = 1/2\, k_B T$, the thermal noise ($z_n$) is given as $\sqrt{\langle z_n^2\rangle} = \sqrt{(k_B T/K)}$. Considering that the noise is due only to the thermal bending motion of the cantilever, the signal-to-noise ratio is given as $z/\sqrt{\langle z_n^2\rangle} = F/\sqrt{(k_B T/K)}$, i.e., proportional to $1/\sqrt{K}$ at any given force [20].

With feedback control, the displacement of the cantilever is counteracted by the radiation pressure and the stiffness is apparently very large. The force is read out from the laser intensity modulation signal, i.e., the feedback voltage (V_{LD}). This signal is proportional to the force that would have generated in the absence of feedback, thus the signal-to-noise ratio remains unchanged. As the feedback magnification is increased, however, other sources of noise cannot be neglected. The total amount of noise in the feedback voltage was greater than the sum of the cantilever's thermal fluctuations and noise in the detector without feedback control. However, in the present experimental condition the noise power below the corner frequency f_C of the servo was almost the same (Fig. 6).

The force data is obtained by removing the high frequency components with a low-pass filter because the time resolution of measurement is determined by the f_C of the cantilever thermal motion (Fig. 6). By operating the feedback system faster than f_C of a cantilever, it is possible to control the position of the lever because the system can detect and control the lever before it moves widely. So large high-frequency components of V_{LD} is not simple noise but is necessary for efficient control of a lever position. The cantilever used in this work, however, was relatively large, so its response to a change in force was slow, 75% rise time was approximately 2 ms and f_C was approximately 100 Hz in solution. In order to obtain better time resolution, the size of the cantilever should ideally be smaller.

Torsional rigidity (C_T) of the glass cantilevers (20 μm × 0.2 μm × 300 μm) is calculated as 5.3×10^{-12} Nm. Average torsional angle of the lever due to thermal motion is obtained as $\sqrt{\langle\theta^2\rangle} = \sqrt{(k_B T/C_T)} = 2.7 \times 10^{-5}$ rad according to the principle of equipartition. Therefore, the displacement at the tip of a stylus (whisker) that have a leg of 10 μm in length by thermal rotating motion is estimated to be 0.3 nm in rms, which is practically small enough for the present experiments. When better resolution is necessary, it is improved by using shorter ZnO crystals.

The ZnO crystal (whisker) used in this work as a probe stylus has a significant advantageous feature that its stylus tip is very sharp, the cone half angle is 1–2° and the radius of curvature at the tip summit is less than 10 nm [14, 15]. Furthermore, the surface of the stylus can be chemically modified by silanization as described here [13]. These characteristics will become very important when intermolecular forces between biomolecules such as protein–protein, protein–lipid and DNA–protein, are measured. A key point with such experiments is how to specifically bind a small number of biomolecules to the probe tip without serious damage to the molecules [21].

To test the performance of our present system, electrostatic repulsive force as a function of the gap distance between positively charged amino groups on the probes and the glass surfaces have been measured (Fig. 8). The force versus distance curves were fitted to a double exponential function. According to the theory of electricity [22], the electrostatic force between a probe stylus and a flat surface (F_e) is given as

$$F_e = a \times \exp(-2\kappa D) + b \times \exp(-\kappa D).$$

Coefficients a and b are described as

$$a = \frac{\pi(\sigma_1^2 + \sigma_2^2)}{\varepsilon_0 \varepsilon_r \kappa^2} [\tan 2\alpha + 2\kappa R + \exp(-2\kappa R) - 1],$$

$$b = \frac{4\pi\sigma_1\sigma_2}{\varepsilon_0 \varepsilon_r \kappa^2} [\tan 2\alpha + 2\kappa R + \exp(-\kappa R) - 1],$$

where κ^{-1} is the Debye length, D is the distance between the stylus tip and the glass surface, σ_1 and σ_2 are the charge density on the glass surface and the stylus surface, respectively, ε_r is the relative dielectric constant of the solution, α is the half angle of the stylus cone, and R is the radius of curvature of stylus spherical end. An α value of 2°, an R value of 10 nm (the upper limit values described in Refs. [14] and [15]) and an ε_r value of 78.0 at 27°C have been used. Calculated κ^{-1} values were 100 ± 18 nm in water (mean ± s.d., $N = 10$, $r = 0.987$), 32 ± 10 nm in 0.1 mM KCl (10, 0.958), 6.4 ± 3.4 nm in 1 mM KCl (6, 0.902), 19 ± 4 nm in 0.1 mM $MgCl_2$ (6, 0.933), and 6.2 ± 1.8 nm in 1 mM $MgCl_2$ (5, 0.927). Correlation coefficient values approaching 1 show that force curves coincide well with the theory of electricity. Fig. 9 shows the dependence of Debye length κ^{-1} upon the bulk concentration of electrolytes. The depend-

ence also coincide well with the Debye–Hückel theory [23], which show the reliability of this novel technique.

Recently, imaging of single fluorescent molecules in solution was achieved [24], and single molecule imaging under scanning probe microscope was also achieved [25]. Intermolecular forces produced by single biological molecules are expected to be in the range of piconewton. The present microscopy has achieved the force sensitivity of sub-piconewton, which is sensitive enough to resolve single molecular forces. In addition, sub-nanometer positioning technique using the feedback system allowed us to keep fragile biological macromolecules away from collapse, which is brought about by contact between the stylus tip and a material surface. Therefore, combination of the present non-contact scanning probe microscopy with the single molecule imaging techniques provides a innovative tool for direct measurement and mapping of intermolecular forces at single molecule level.

5. Conclusions

We have improved the force resolution of AFM to sub-piconewton level by using very flexible handmade cantilevers. Thermal bending motions of the cantilevers were reduced to less than 1 nm in rms by exerting feedback positioning with laser radiation pressure. Sub-piconewton intermolecular forces were resolved at controlled gaps between the probe and a material surface in the nanometer range. These levels of force sensitivity and position control meet the requirements needed for two-dimensional imaging of intermolecular forces between biomolecules such as protein–protein, protein–lipid, ligand–receptor and protein-DNA pairs.

Acknowledgements

We thank M. Kitano, H. Kado and H. Ogawa (Matsushita) for the gift of ZnO whiskers; A. Ishijima and H. Tanaka (ERATO) for the gift of chemical-etched glass coverslips; Y. Hasebe and K. Nakai (Sentech) for technical support of the feedback circuit; Y. Hayashi and A. Yagi (Olympus) for technical support of AFM; T. Wakabayashi (Asahi Glass) for silane chemistry; and J. West (Monash Univ.) for critical reading of the manuscript. This work was partially supported by JSPS Research Fellowships for Young Scientists (T. A.).

References

[1] G. Binnig, C.F. Quate, Ch. Gerber, Phys. Rev. Lett. 56 (1986) 930.
[2] C. Bustamante, D. Keller, Physics Today (December 1995) 32.
[3] E.-L. Florin, V.T. Moy, H.E. Gaub, Science 264 (1994) 415.
[4] A. Chilkoti, T. Boland, B. Ratner, P.S. Stayton, Biophys. J. 69 (1995) 2125.
[5] G.U. Lee, L.A. Chrisey, R.J. Colton, Science 266 (1994) 771.
[6] M. Radmacher, M. Fritz, H.G. Hansma, P.K. Hansma, Science 265 (1994) 1577.
[7] N.H. Thomson, M. Fritz, M. Radmacher, J.P. Cleveland, C.F. Schmidt, P.K. Hansma, Biophys. J. 70 (1996) 2421.
[8] A. Ishijima, T. Doi, K. Sakurada, T. Yanagida, Nature 352 (1991) 301.
[9] K. Svoboda, C.F. Schmidt, B.J. Schnapp, S.M. Block, Nature 365 (1993) 721.
[10] J.T. Finer, R.M. Simmons, J.A. Spudich, Nature 368 (1994) 113.
[11] A. Ishijima, H. Kojima, H. Higuchi, Y. Harada, T. Funatsu, T. Yanagida, Biophys. J. 70 (1996) 383.
[12] H. Yin, M.D. Wang, K. Svoboda, R. Landick, S.M. Block, J. Gelles, Science 270 (1995) 1653.
[13] M. Tokunaga, T. Aoki, M. Hiroshima, K. Kitamura, T. Yanagida, Biochem. Biophys. Res. Commun. 231 (1997) 566.
[14] H. Kado, K. Yokoyama, T. Tohda, Ultramicroscopy 42–44 (1992) 1659.
[15] H. Kado, K. Yokoyama, T. Tohda, Rev. Sci. Instrum. 63 (1992) 3330.
[16] M. Kitano, T. Hamabe, S. Maeda, T. Okabe, J. Crystal Growth 102 (1990) 965.
[17] A. Kishino, T. Yanagida, Nature 334 (1988) 74.
[18] R. Kaneko, S. Oguchi, S. Hara, R. Matsubara, T. Okada, H. Ogawa, Y. Nakamura, Ultramicroscopy 42–44 (1992) 1542.
[19] R.M. Simmons, J.T. Finer, S. Chu, J.A. Spudich, Biophys. J. 70 (1996) 1813.
[20] T. Yanagida, Y. Harada, A. Ishijima, TIBS 18 (1993) 319.
[21] A.H. Iwane, K. Kitamura, M. Tokunaga, T. Yanagida, Biochem. Biophys. Res. Commun. 230 (1997) 76.
[22] H.-J. Butt, Biophys. J. 60 (1991) 777.
[23] J.N. Israelachvili, Intermolecular and Surface Forces, Academic Press, London, 1985.
[24] T. Funatsu, Y. Harada, M. Tokunaga, K. Saito, T. Yanagida, Nature 374 (1995) 555.
[25] M. Tokunaga, K. Kitamura, K. Saito, A.H. Iwane, T. Yanagida, Biochem. Biophys. Res. Commun., in press.